CHAPTER 6

PHASE CHANGES IN A MODEL SUPERALLOY

6.1 Introduction

Nimonic alloy PE16 (e.g. Henry Wiggin Ltd. 1968[1971]; Raynor and Silcock 1970; Bramman, Fraser and Martin 1971; Silcock 1971; Raynor 1971; Sims and Hagel 1972; Betteridge and Heslop 1974; Nembach 1974; Martens and Nembach 1975; Faulkner and Caisley 1977; White and Fisher 1978), originally developed as a weldable structural material, has high projected potential in the nuclear industry as a fuel cladding material because it is stable to both radiation enhanced coarsening and void swelling.

These phenomena of stability are not understood completely as yet. The model alloy examined in the present study (composition in Table 6.1) is taken from a series of materials designed by Shaw (Shaw 1980) in order to investigate the relationship between one possible key factor, the composition of the γ' phase, and stability of the γ/γ' microstructure. In all cases the models simulate the matrix of PE16 but changes are made in the content and relative balance of the γ'-formers. The particular aim of this atom probe investigation is to determine, initially for one key alloy, the mechanism and kinetics of γ' precipitation and, on an atomic scale, associated partitioning and segregation effects.

6.2 Results

Table 6.1. Compositional Data for PE16-type alloys: 6 major elements

	Al/wt%	Ti/wt%	Ni/wt%	Cr/wt%	Fe/wt%	Mo/wt%
Henry Wiggin Ltd. PE16 Spec. DTD 5047 (Wiggin 1971)	0.9 -1.5	0.9 -1.5	42.0 -45.0	15.0 -18.0	bal.	2.5 -4.0
Matrix Model Alloy Nominal.	1.11	1.12	35.3	17.6	39.2	4.85
APFIM Analysis of Matrix Model.	1.41 ±0.09	1.72 ±0.15	34.02 ±0.72	17.42 ±0.52	41.30 ±0.77	4.43 ±0.33

Table 6.2. QAP Analyses of PE16 Matrix Model: Matrix Phase

Heat Treatment	Al/at%	Ti/at%	Ni/at%	Cr/at%	Fe/at%	Mo/at%
Homogenised	3.16 ±0.09	1.72 ±0.07	31.74 ±0.32	17.74 ±0.10	43.25 ±0.33	2.40 ±0.08
900°C, 1 hour	2.22 ±0.08	0.62 ±0.04	35.20 ±0.33	16.45 ±0.23	43.59 ±0.37	1.92 ±0.08
750°C, 20 mins.	2.27 ±0.11	0.47 ±0.05	32.00 ±0.43	17.79 ±0.32	45.31 ±0.51	2.17 ±0.11
750°C, 2 hours	2.30 ±0.08	0.38 ±0.03	31.27 ±0.31	21.36 ±0.26	41.93 ±0.36	2.75 ±0.09
750°C, 4 hours	2.09 ±0.07	0.42 ±0.03	30.47 ±0.27	19.81 ±0.22	44.84 ±0.33	2.37 ±0.08
750°C, 8 hours	2.51 ±0.12	0.41 ±0.05	27.39 ±0.39	22.23 ±0.36	45.03 ±0.50	2.43 ±0.12

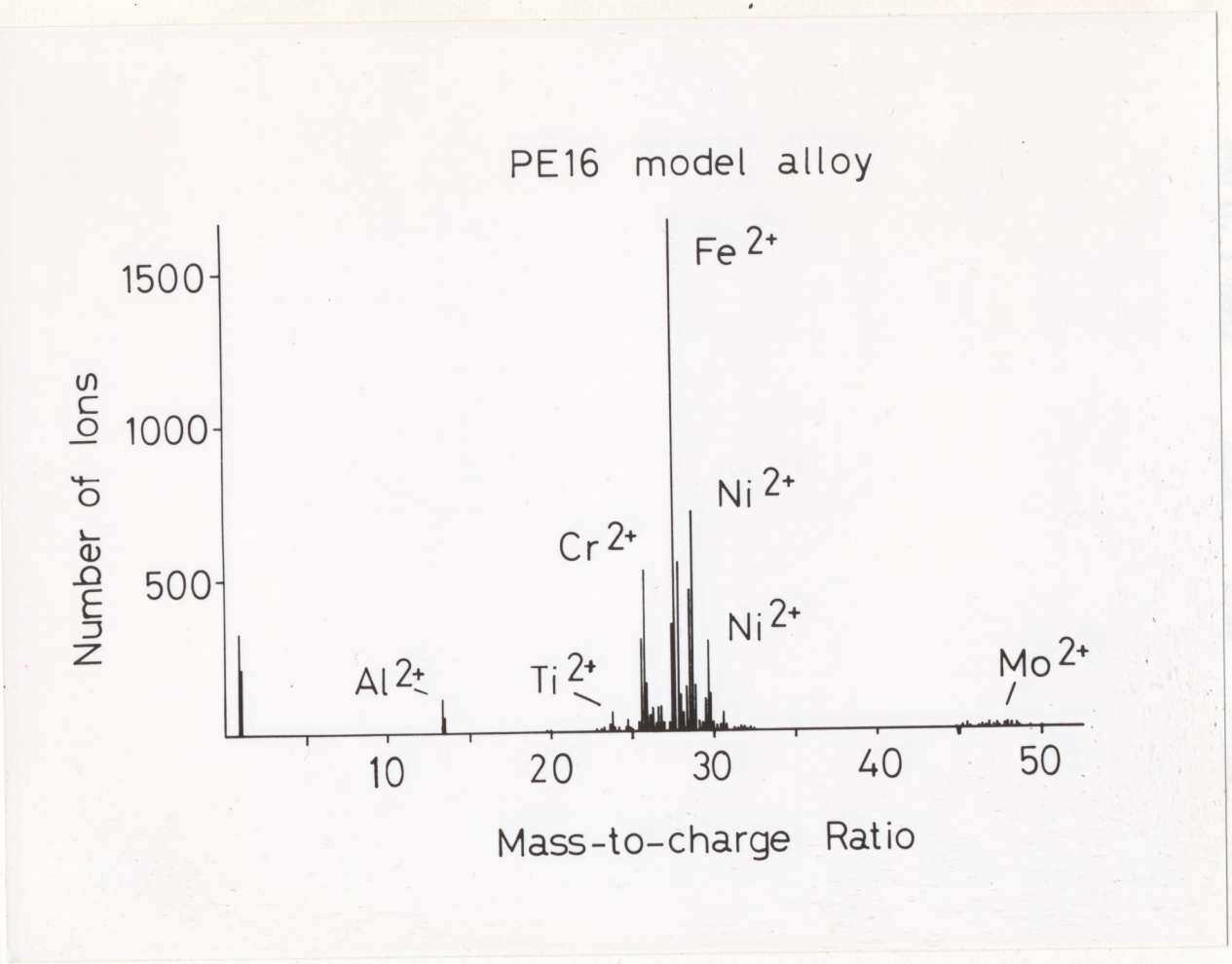

Figure 6.1 Mass spectrum from the PE16 matrix model.

6.2.1 Solution and carbide treatments

Solution-treated specimens (1050°C, 2 hour) exhibited no evidence of inhomogeneity: IAP examination showed uniform distributions of all six major alloying elements and QAP traces revealed only random statistical fluctuations in composition. The overall composition determined by QAP analysis (Table 6.1 and also Table 6.2) agreed well with the nominal value, with the possible exceptions of the aluminium and titanium contents which were slightly higher than anticipated. A mass spectrum from the alloy is presented in figure 6.1.

Similar observations of intragranular homogeneity were made after carbide precipitation treatment (900°C, 1hour), with the exception of a single, small intragranular carbide particle encountered in one QAP experiment; i.e., no γ' precipitation occurred during the air cool. Composition determination revealed, however, that depletion of aluminium, titanium, chromium and molybdenum had occurred (Table 6.2).* With respect to the carbide particle, insufficient data were collected for accurate compositional analysis, but it was noted that chromium and carbon contents were significantly enriched, and nickel

*It should be noted that throughout this chapter composition measurements refer only to intragranular regions. These values may differ from the true overall alloy composition by an amount determined by the nature and extent of grain-boundary phases.

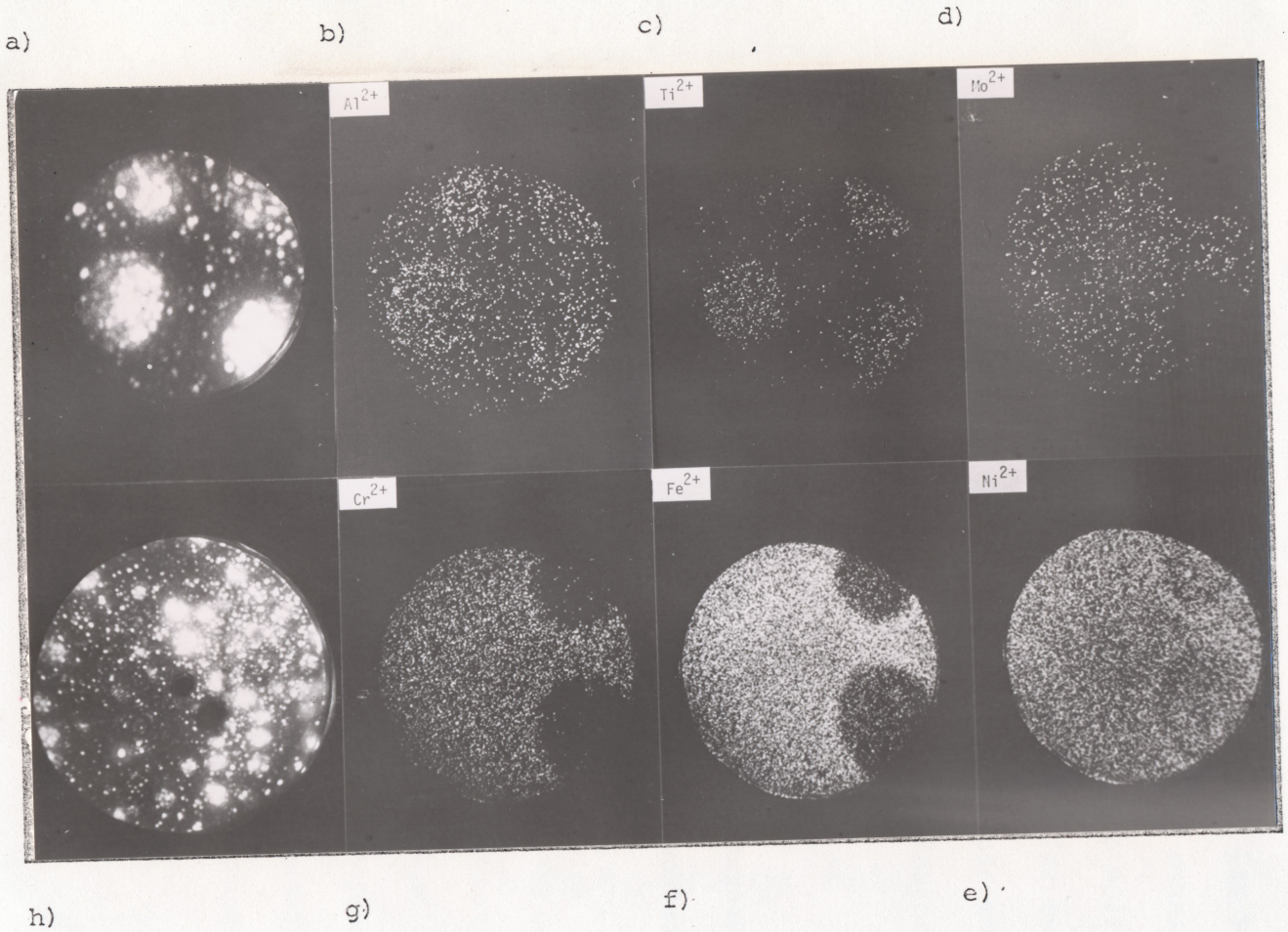

Figure 6.2 APFIM micrographs of PE16 matrix model after 8 hours ageing at 750°C. a) and h) FIM images. b) Al^{2+}, c) Ti^{2+}, d) Mo^{2+}, e) Ni^{2+}, f) Fe^{2+}, g) Cr^{2+}.

depleted. No grain boundary carbides were examined.

6.2.2 γ' precipitation I: qualitative observations

6.2.2i General precipitation: FIM

After the first ageing period of 20 minutes at 750°C small, spherical and ordered particles of γ' were visible in the field-ion image. Careful examination of γ' ring structures in several series of field-ion micrographs revealed no dislocations upon which the second phase might have nucleated heterogeneously.

Upon further ageing for periods of up to eight hours the precipitates increased in size but remained spherical. Observations of several micrographs for each heat treatment suggested that the particles were randomly distributed.

6.2.2ii General partitioning and segregation: IAP and QAP

Time-gated IAP microscopy of material aged for 20 minutes revealed preferential partitioning of nickel, aluminium and titanium to the γ' phase, and accumulation of iron, chromium and molybdenum in the matrix. Further rejection from the γ' lattice of most of the remaining chromium, iron, and molybdenum occurred as the ageing period was extended.

The micrographs of figure 6.2 illustrate the features of this partitioning after eight hours. Figures 6.2b-g show consecutive IAP

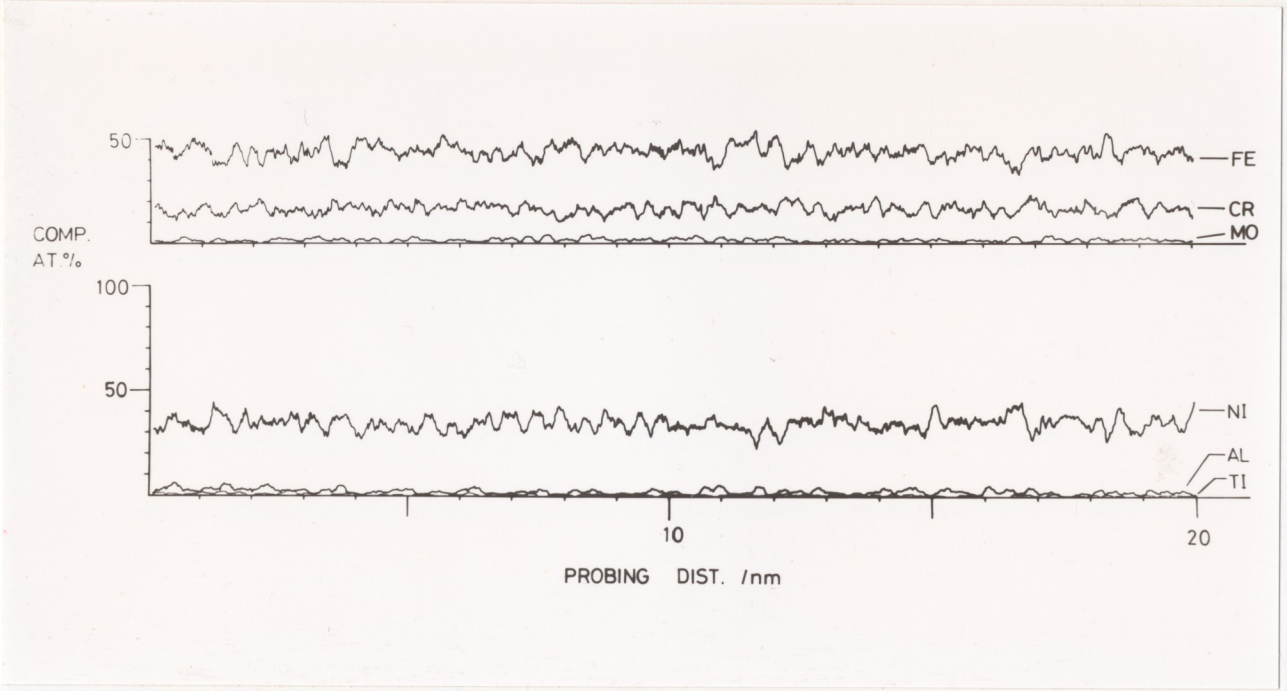

Figure 6.3a QAP trace from a carbide-treated specimen (900°C, 1 hour, air-cooled).

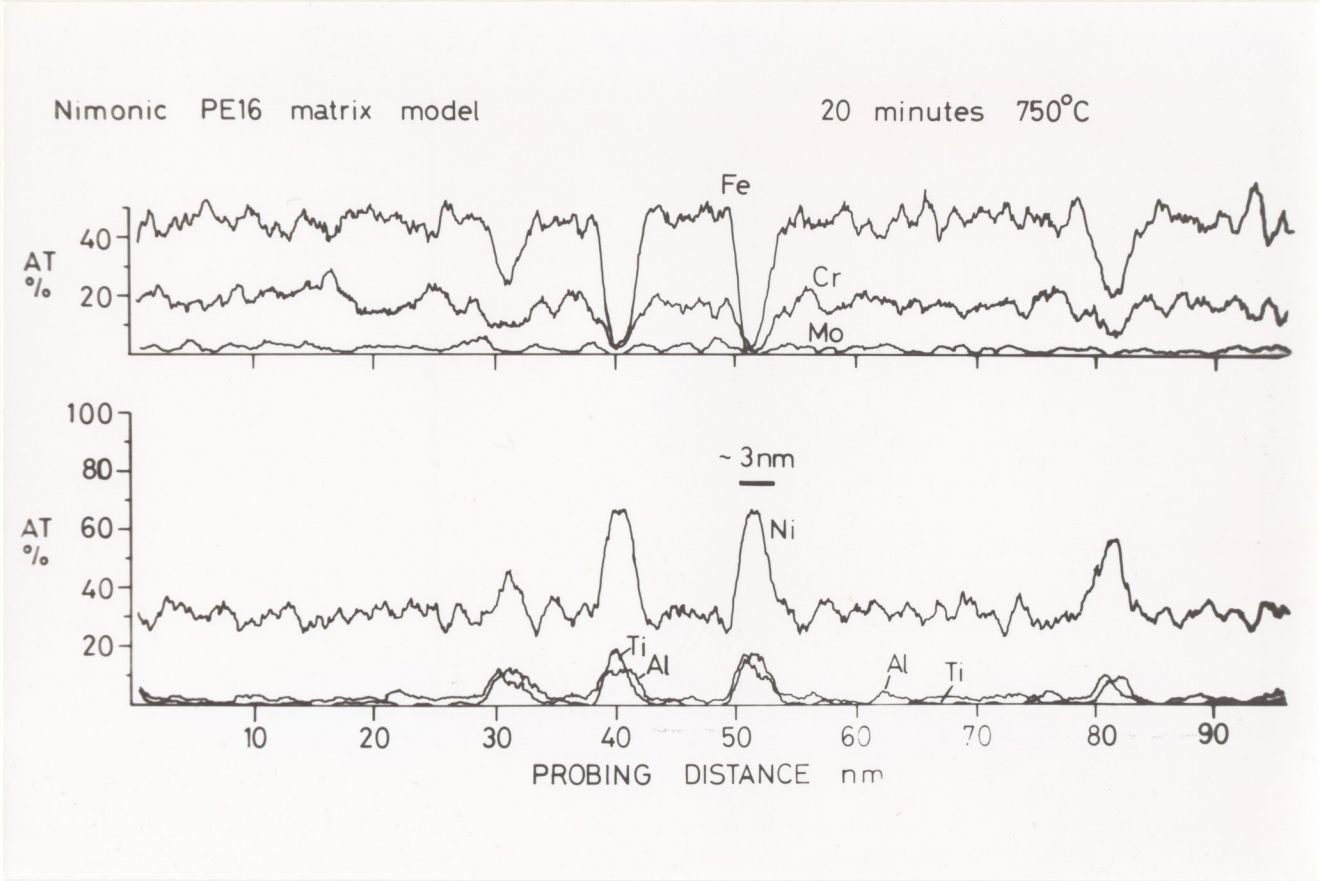

Figure 6.3b QAP trace after an additional 20 minutes at 750°C.

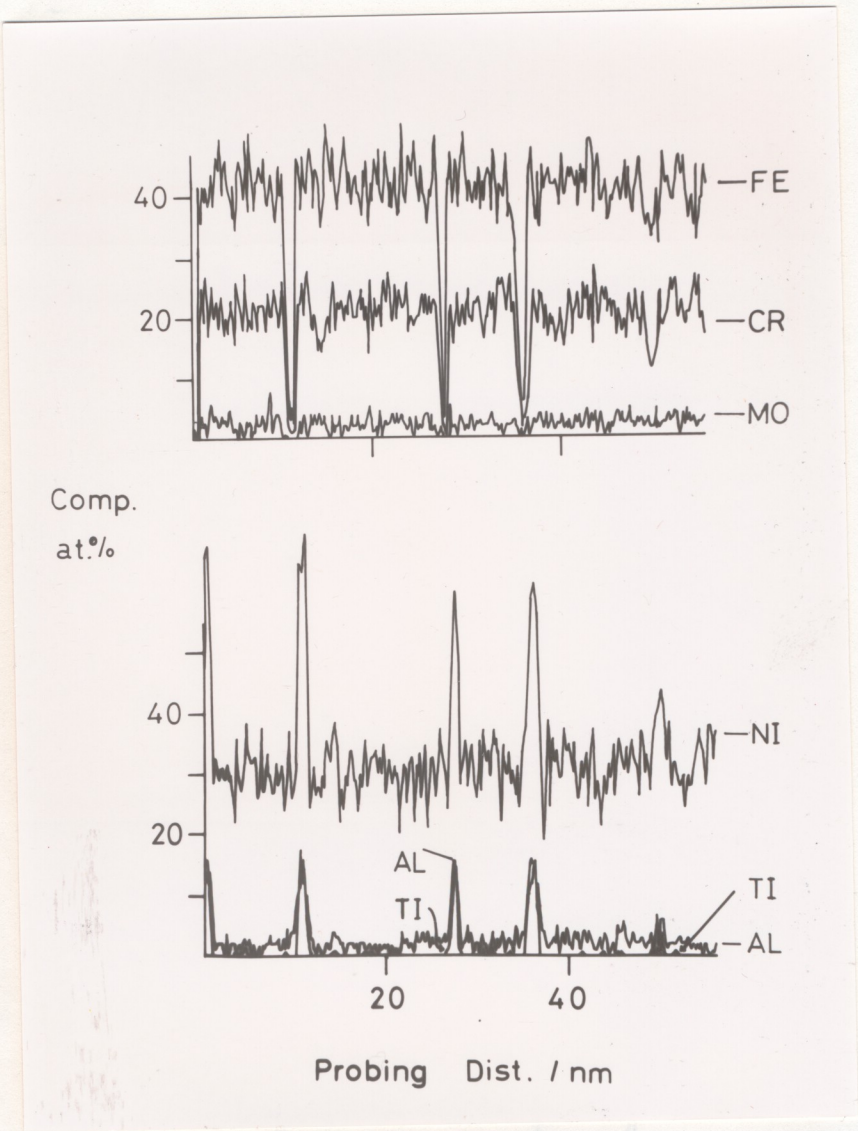

Figure 6.3c QAP trace after 2 hours at 750°C.

images, taken in the order Al^{2+} (b), Ti^{2+} (c), Mo^{2+} (d), Ni^{2+} (e), Fe^{2+} (f), Cr^{2+} (g), from the area shown in figure 6.2a. Each image is integrated over approximately five atomic planes. Not all precipitates which were intersected initially persisted throughout the sequence, but in those which did so preferential partitioning of aluminium, nickel and titanium to the γ' is evident, with traces of iron, chromium and molybdenum. Sharpness of the particle/matrix interface should also be noted.

The final field-ion micrograph, figure 6.2h, shows an overall view of the two-phase microstructure.

These results were confirmed by QAP analysis. Figure 6.3 presents three typical QAP traces illustrating a) the reference state of a carbide-treated sample, b) γ' precipitation after 20 minutes ageing time at 750°C (high degree of partitioning), and c) the smaller changes in γ and γ' compositions after 2 hours ageing. In particular it should be noted that the total (Al + Ti) level in the regions of maximum composition excursion approximates to 25 at.%, as required for the $Ni_3(Al,Ti)$ structure. The lack of γ' precipitation during the air cool from the carbide treatment suggests that second phase separation requires an incubation time i.e. that the new phase is nucleated rather than generated continuously. Thus any small compositional excursions observed on the APFIM traces may be be attributed to simultaneous sampling of γ and γ' regions, rather than to genuine low-amplitude compositional modulations, and are disregarded in analyses. The precipitation mechanism is discussed in more detail in Section 6.3.1.

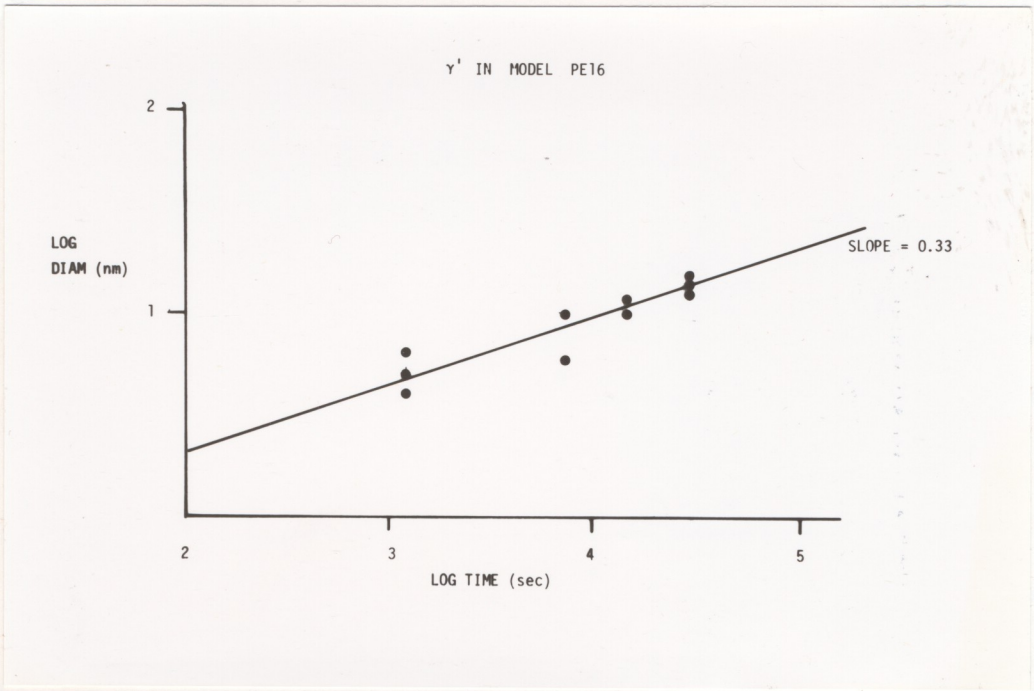

Figure 6.4 Plot of log(particle diameter) vs. log(time) for PE16 matrix model alloy.

Further close examination of QAP profiles also showed that at all ageing times the particle/matrix interface was reasonably sharp, extending over 3-4 atomic planes. No evidence of interfacial segregation was found and no large solute-depleted zones around γ' particles were observed. It was also noted that the interface width was the same for all diffusing species in all interfaces studied (~100).

6.2.2iii Semi-quantitative observations

Some estimates of particle size after each ageing treatment were obtained from IAP images (allowing for effects such as image compression) and from precipitate intersections on QAP traces (for methods of accurate analysis see e.g. Schwartz and Ralph 1969, 1970). The results are shown plotted as log(diameter) against log(time) in figure 6.4. This graph is linear with a best-fit slope of approximately 0.3 i.e.

$$d = k_3 t^{1/3}$$

The volume fraction of precipitate was estimated as 5-10 % for all ageing times.

6.2.2iv Subsidiary data: X-ray and TEM studies

X-ray diffraction studies of specimens of all heat-treatments revealed cubic F reflections of lattice parameter 0.356 nm, with no strain broadening. Specimens containing γ' particles also gave weak

Further close examination of QAP profiles also showed that at all ageing times the particle/matrix interface was reasonably sharp, extending over 3-4 atomic planes. No evidence of interfacial segregation was found and no large solute-depleted zones around γ' particles were observed. It was also noted that the interface width was the same for all diffusing species in all interfaces studied (~100).

6.2.2iii Semi-quantitative observations

Some estimates of particle size after each ageing treatment were obtained from IAP images (allowing for effects such as image compression) and from precipitate intersections on QAP traces (for methods of accurate analysis see e.g. Schwartz and Ralph 1969, 1970). The results are shown plotted as log(diameter) against log(time) in figure 6.4. This graph is linear with a best-fit slope of approximately 0.3 i.e.

$$d = k_3 t^{1/3}$$

The volume fraction of precipitate was estimated as 5-10 % for all ageing times.

6.2.2iv Subsidiary data: X-ray and TEM studies

X-ray diffraction studies of specimens of all heat-treatments revealed cubic F reflections of lattice parameter 0.356 nm, with no strain broadening. Specimens containing γ' particles also gave weak

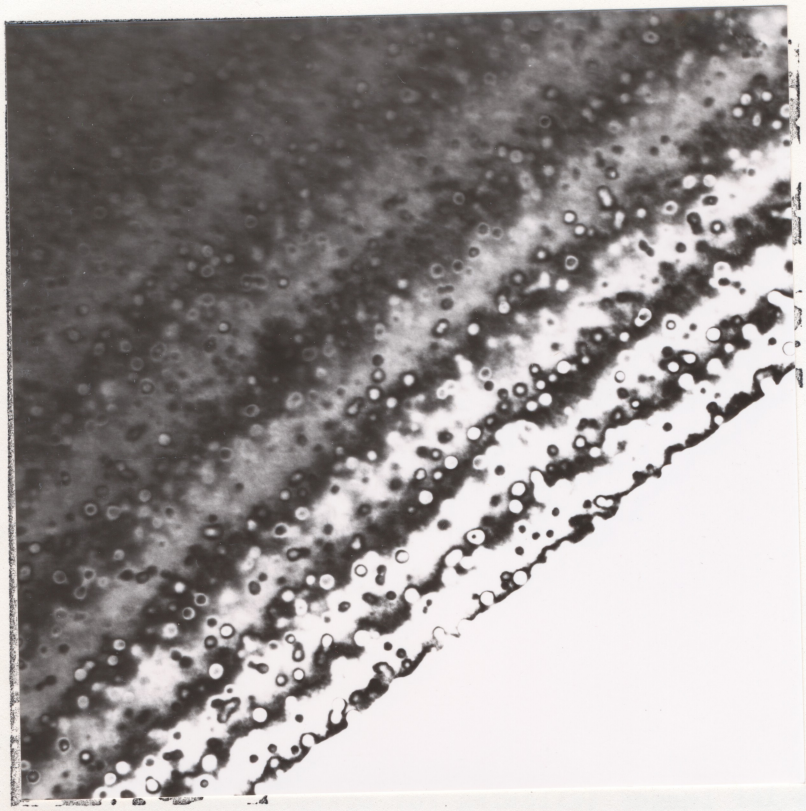

Figure 6.5 Bright-field transmission electron micrograph of the matrix model after 8 hours ageing at 750°C (courtesy of Dr. M. P. Shaw).

Table 6.3. QAP Analyses of PE16 Matrix Model: γ' Phase

Heat Treatment	Al/at%	Ti/at%	Ni/at%	Cr/at%	Fe/at%	Mo/at%
750°C, 20 mins.	12.40 ±0.64	13.10 ±0.66	58.68 ±1.40	5.53 ±0.33	9.72 ±0.57	0.57 ±0.14
750°C, 2 hours	14.15 ±0.85	14.20 ±0.85	62.26 ±1.79	2.36 ±0.35	6.15 ±0.56	0.87 ±0.21
750°C, 4 hours	11.08 ±0.32	12.23 ±0.34	72.64 ±0.82	1.45 ±0.12	2.50 ±0.15	0.09 ±0.03
750°C, 8 hours	9.99 ±0.42	16.28 ±0.54	68.96 ±1.11	1.94 ±0.19	2.77 ±0.22	0.07 ±0.04

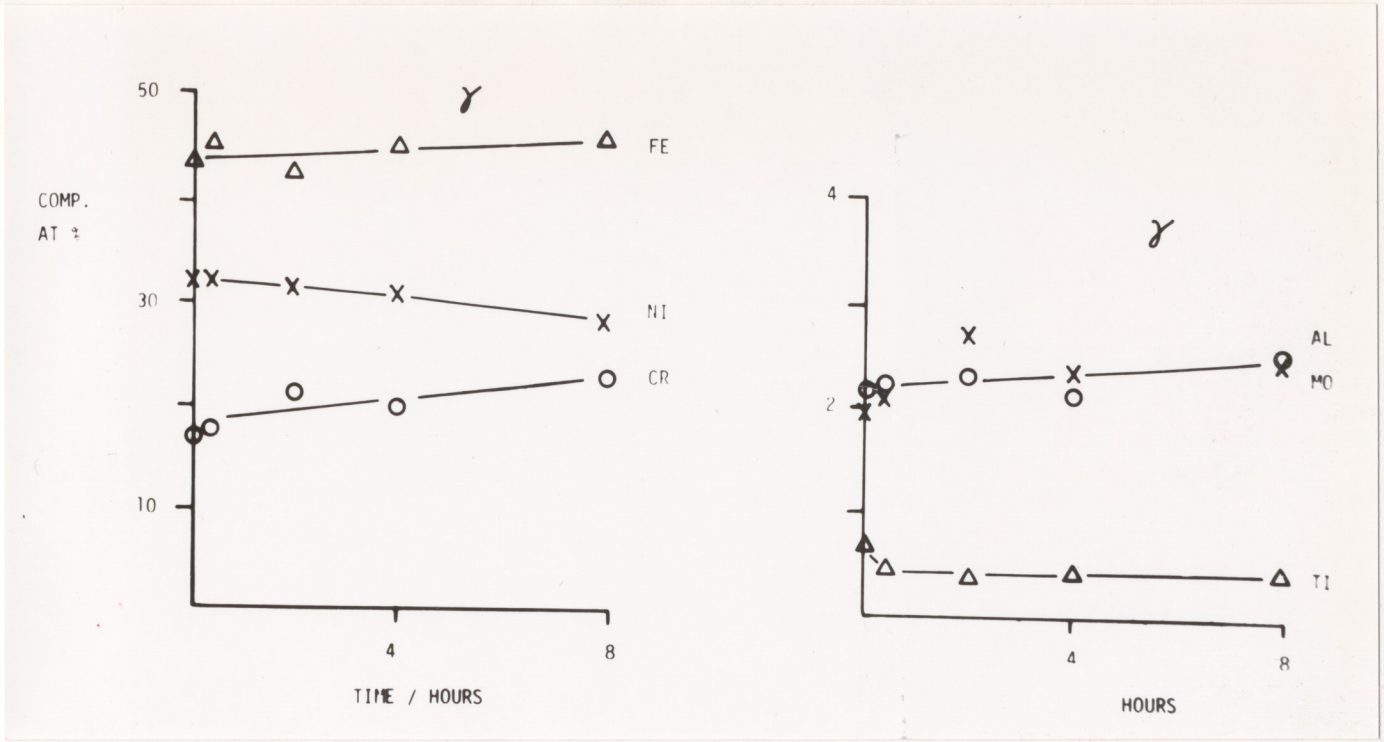

Figure 6.6 Composition of matrix phase as a function of ageing time.

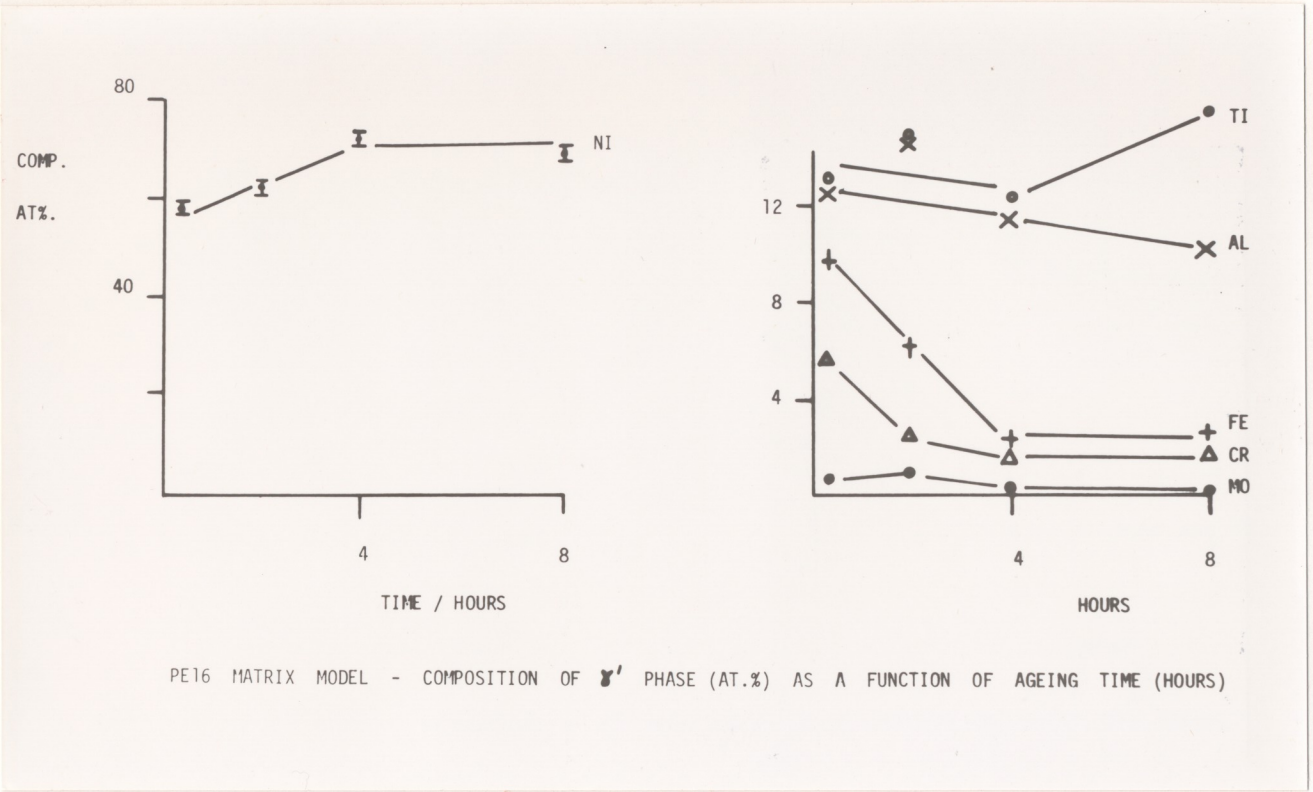

PE16 MATRIX MODEL - COMPOSITION OF γ' PHASE (AT.%) AS A FUNCTION OF AGEING TIME (HOURS)

Figure 6.7

cubic P reflections of the same lattice parameter. TEM studies (Shaw 1980) confirm that only small strain fields exist in the two-phase microstucture.

Figure 6.5 (courtesy Shaw) shows a bright-field TEM image taken from a specimen aged for 8 hours at 750°C. The γ' phase is present as spheres of apparently random distribution. The volume fraction is approximately 8%, and particle diameters are in the range 12-18 nm, which agrees well with estimates from atom-probe microscopy.

6.2.3 γ' precipitation II: quantitative compositional analysis by QAP

Compositional determinations for the γ and γ' phases at each stage of heat treatment were effected by summation of ion counts for each element over a number of matrix and precipitate regions. The results of these analyses are displayed in Tables 6.2 (γ) and 6.3 (γ'), with error estimates derived using the relation error= $(nc)^{\frac{1}{2}}/n$, where n is the number of readings and c the calculated atom fraction. The values are plotted respectively as a function of ageing time in figures 6.6 and 6.7.

Looking first at the matrix phase (figure 6.6), it may be seen that iron, chromium and molybdenum behave similarly, showing a slight rise in concentration after 20 minutes ageing, and then tending towards a plateau with longer heat treatment. Aluminium and titanium conversely exhibit a rapid initial drop in concentration with 900°C ageing and initial 750°C treatments, before reaching an approximate plateau. Nickel is depleted slowly throughout the ageing sequence.

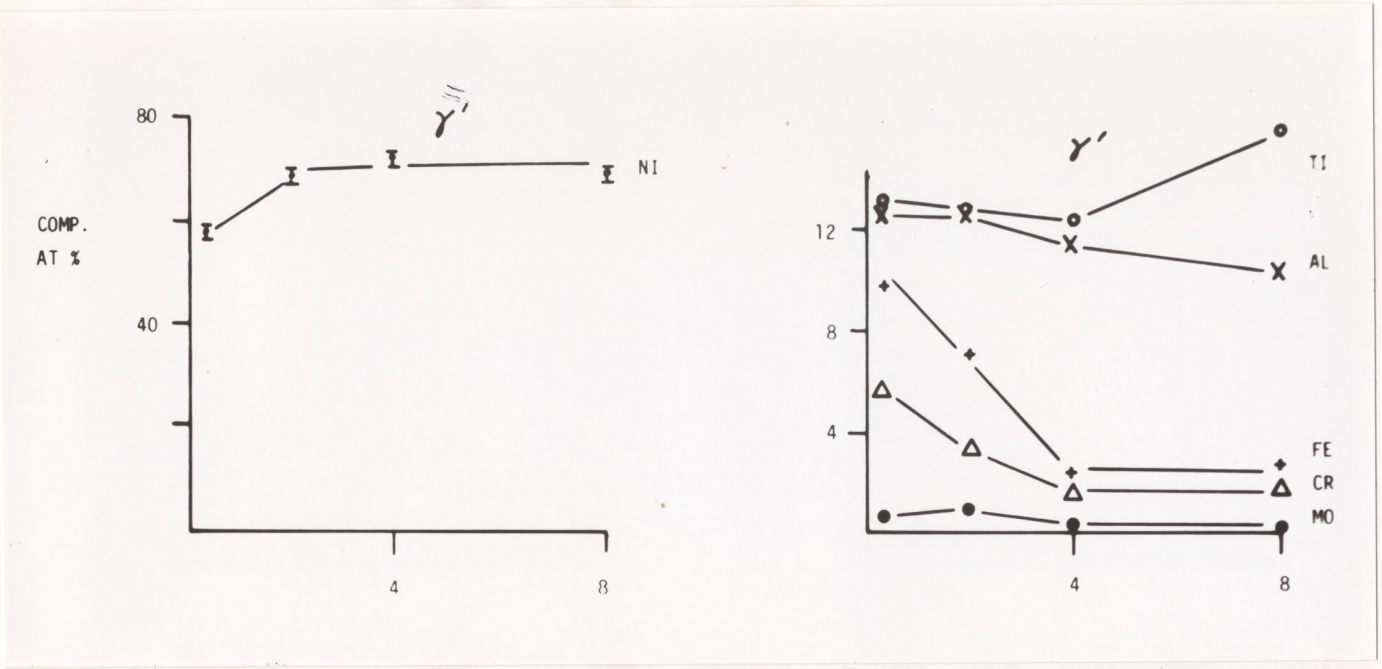

Figure 6.8 Composition of γ' phase as a function of ageing time with corrected data for 2 hours ageing.

Turning to the γ' phase (figure 6.7), attention is drawn to the behaviour of aluminium and titanium. Throughout the γ' treatments studied, the sum total of these two elements remains approximately constant at the stoichiometric level. However, the relative proportion of each is apparently a function of ageing time: for the first four hours of ageing the elements are present in approximately equal amounts (Al/Ti=1.1±0.05), but after eight hours the titanium content is increased significantly at the expense of aluminium, to give an overall Ti:Al ratio of approximately 1.6±0.05.

The remaining elements show trends which are the reverse of those in the γ phase. Iron, chromium and molybdenum, present at concentrations of a few atomic percent after 20 minutes, are rejected to reach low plateau levels after four hours, while nickel is significantly enriched. It may be noted that molybdenum shows a particularly low residual level of ~0.1 at.%.

It may also be observed that the γ' compositions derived for 2 hours ageing are apparently slightly anomalous, with aluminium and titanium contents well above stoichiometric values. Examination of laboratory records showed that the readings had been taken at a low detection rate, necessitating long waiting periods at standing voltage. Under such circumstances, and others such as hydrogen etching or low pulse-to-standing voltage ratio, apparent loss of nickel (i.e. enrichment of Al and Ti) has been noted in other experiments. The γ' data for 2 hours ageing have thus been adjusted to the correct aluminium and titanium content, and are shown replotted in figure 6.8. This change certainly improves agreement with

projected behaviour and reinforces general trends.

QAP measurements of partitioning may also be used to estimate the volume fraction of precipitated γ' phase, given the aluminium and titanium concentrations in carbide-treated alloy as a reference state. For material aged for 4 hours such calculations give a value of 11-12 %, assuming that all aluminium and titanium lost from the matrix is accomodated in stoichiometric γ'. This estimate is somewhat higher than those derived from micrographs, but it is most certainly an overestimate, as some aluminium and titanium will be lost not only to γ', but also to carbides, and also from the specimen surface during heat treatment.

6.3 Discussion

6.3.1 Phase Transformations

6.3.1i Precipitation

The specific observation of lack of γ' precipitation during air-cool from 950°C , i.e. the existence of an incubation time for the reaction, suggests that the γ' phase is generated by nucleation and not by continuous change (see section 6.2.2ii above). The random distribution of the second phase, and the absence of dislocations within the particles, suggests that the nucleation may be homogeneous. This may be anticipated with zero γ/γ' lattice mismatch (e.g. X-ray analyses). Heterogeneous nucleation on vacancies is not ruled out on this basis, but it is most unlikely that sufficient vacancy sites

would remain after an anneal at 950°C. The effect of other point defects could not be assessed.

It may be demonstrated using the Cook-Hilliard (1965) analysis for the chemical spinodal (see Chapter 4) that a conventional nucleation mechanism is to be expected given that the volume fraction of γ' phase has been measured at 8-10 %. It should first be noted that the present system shows no lattice mismatch between precipitate and matrix. Thus the chemical and coherent spinodals may be assumed to be coincident. Recalling the Cook - Hilliard equation (E4.1)

$$C_s - C_c = C_e - C_c \left[1 - 0.422 \, (T/T_c) \right]$$

this analysis calculates the ratio $(C_s - C_c)/(C_e - C_c)$ for two phases with knowledge only of T_c. Setting T_c to a reasonable value of 1200°C for PE16, and assuming a pseudo-binary system of a matrix of (Ni, Cr, Fe, Mo) (γ) and of a precipitate (Ni_3(Al,Ti)) (γ'), $(C_s - C_c)_{750°C}$ is found to be 0.71 $(C_e - C_c)$, i.e. the spinodal occurs at a volume fraction of approximately 30% γ'. This is well above the measured fraction.

It was also observed that the precipitates were at least partially ordered after 20 minutes ageing, but no details of the ordering mechanism were established.

6.3.1ii Coarsening

The test of coarsening kinetics in figure 6.3 appears to show quite clearly that spherical γ' particles obey the $t^{1/3}$, L-S-W, or

volume diffusion controlled coarsening law (Chapter 2), within the ageing range 20 minutes-8 hours. That VDC ripening is observed implies that precipitation is fully accomplished within 20 minutes or less. These observations are in full agreement with those of Silcock 1970 for commercial PE16.

Observations of a constant (Al+Ti) ratio of 25 at.% in the γ' phase, sharp interfaces between precipitate and matrix, and approximately equal interface width for all elements are consistent with phenomena of nucleation and subsequent growth under VDC.

6.3.2 Partitioning

Considering first the effect of carbide treatment on the model microstructure, QAP analysis shows major elemental losses for aluminium and titanium, and smaller decreases in chromium and molybdenum. Small compositional changes by carbide formation are certainly to be expected for the latter three elements, but depletion of aluminium and the large similar effect for titanium probably indicate loss by surface activity (evaporation or oxidation) during heat treatment.

In summary of the general γ/γ' partitioning behaviour, iron, chromium and molybdenum accumulate in the matrix with ageing and nickel, aluminium and titanium collect preferentially in the γ'. This is fully consistent with the general behaviour of superalloys, as discussed in Chapter 1. A few examples of other determinations of partitioning, using various methods, are: Kriege and Baris (1969) and

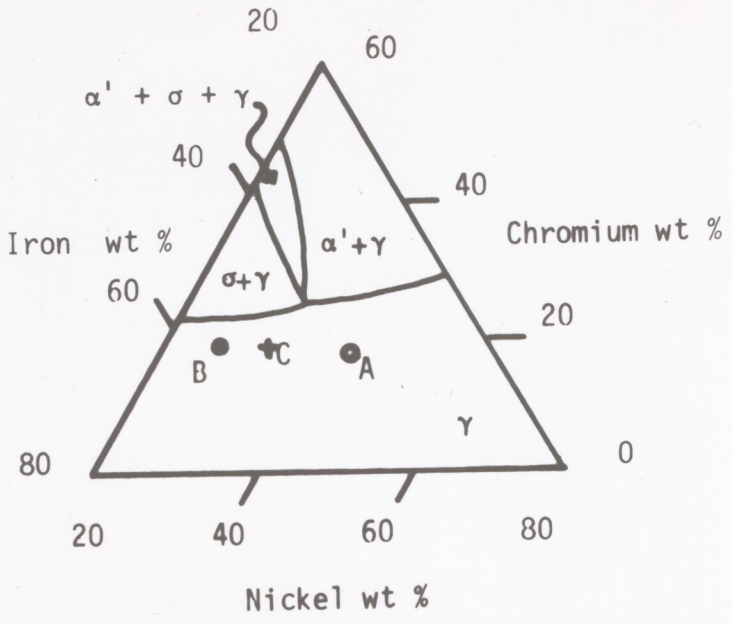

PE16 on the Ni-Fe-Cr ternary diagram.

A - overall composition

B - matrix composition (PHACOMP)

C - matrix composition, present analysis

Figure 6.9 Further calculation of the location of Nimonic PE16 on the Ni-Fe-Cr ternary diagram.

Shimanuki, Masui and Doi (1976) (wet analyses); Beaven, Miller and Smith (1977), Beaven, Delargy, Miller and Smith (1978) and Wood, Mills, Waugh and Bee (1980) (APFIM); and Howell and Bee (1980) (STEM).

More detailed partitioning analyses by QAP confirm that approximately complementary elemental behaviours occur in γ and γ' phases. Compositional changes are thus discussed only in terms of γ' results. One note concerning the γ phase may be made, however. Using the mean elemental concentrations determined by QAP analysis the position of the matrix on the nickel-chromium-iron phase diagram for PHACOMP (see Chapter 1 above) has been reestimated. In figure 6.9 the new value (C) is shown on a section of the nickel-chromium-iron diagram similar to that of figure 1.1. The position of the overall alloy composition and the PHACOMP estimate of the residual matrix composition are shown respectively as points A and B. In constructing point B PHACOMP assumes that the major γ'-forming elements aluminium and titanium partition completely to the second phase. In practice these two elements possess some solubility in the matrix, as has been shown in the present APFIM study. Thus some disparity is to be expected between the PHACOMP estimate of composition and the measured value, C. However, it should be noted that the matrix is still close to σ separation and that PHACOMP gives a good approximation to true behaviour in this respect.

Specifically concerning the γ' phase, iron, chromium and molybdenum are present after 20 minutes of ageing, at an approximate total level of 15-16 at.%, but are rejected to a residual total content of approximately 5 at.% after 4 hours. Nickel is

simultaneously enriched from 58-59 at.% to around 70 at.%. Given also that the (Al + Ti) content is maintained at ~25 at.% throughout this readjustment, these results would appear to substantiate the observation in Chapter 1 that chromium, iron and molybdenum act as substituents for nickel. However, on this information alone, it cannot be concluded that these elements occupy only nickel sub-lattice sites.

The (Al + Ti) content also remained at ~25 at.% between 4-8 hours of ageing. However, during this period, and thus apparently subsequent to the rejection of chromium, etc., the Ti/Al ratio was adjusted from 1.1±0.06 to 1.6±0.05. General enhancement of the γ' Ti/Al ratio (and loss of chromium) has been observed previously in a quaternary nickel-iron-titanium-aluminium alloy by Rogen and Grant 1960. In this latter case it was also suggested that the period of enrichment also coincided with an arrest in the coarsening curve, but no such ripening plateau was observed in the present studies. It has been suggested that chromium impedes ordering of the γ' lattice (Ham 1970; Wood, Mills, Waugh and Bee 1980). Present results certainly suggest that lattice rearrangement may be subject to low chromium concentration. This remains to be confirmed.

Overall the findings of homogeneous nucleation with random particle distribution and L-S-W coarsening are consistent with theoretical expectations. These properties are in contrast to those of the microstructurally modulated and rapidly-coarsening materials of high lattice mismatch and high volume fraction of second phase.

Direct relationships between this model and commercial PE16 are to be treated with caution. However, it may be noted that the enrichment of Ti/Al ratio in the model alloy corresponds in ageing time to the development of optimum hardening in the commercial alloy. It remains to be established whether similar enrichment occurs in the latter. However, if this were so the result would support the suggestion of Phillips (1968) that in the absence of lattice strain precipitation hardening by γ' depends upon high Ti/Al ratio in the precipitates However, before firm conclusions may be drawn concerning this hardening effect, the partitioning must be followed to longer ageing times in order to establish that no further change occurs. Subsequent alloys in the Shaw 1980 series may then be investigated in order to ascertain the effects of changing the γ' composition.

6.4 Summary

It has been shown that the γ' phase is generated in the experimental alloy by a conventional nucleation mechanism. No evidence of heterogeneous processes was observed. Coarsening of the spherical second phase obeys a $t^{1/3}$ coarsening law. QAP analyses of elemental partitioning between γ and γ' phases showed that iron, chromium and molybdenum are rejected from γ' upon ageing to leave low residual levels after 4 hours. At all times the sum total of (aluminium + titanium) in the γ' approximates to 25 at.%. However, subsequent to achievement of the equilibrium iron, chromium, and molybdenum levels, the Ti/Al ratio in the γ' phase is adjusted from 1.1 ± 0.06 to 1.6 ± 0.05. This corresponds in ageing time to development of optimum hardening in the commercial alloy and it has been suggested

that the relationship between γ' composition and hardness should be examined further.